Effect of Functionally Graded Material of Spacer with Contaminating Particle on Breakdown Voltage inside Gas Insulated Bus Duct

Sayed A. Ward, M. A. Abd Allah, Amr A. Youssef

Abstract— For the enhancement of insulation reliability and the compact design in gas insulated power equipment, the solid insulators play crucial role of electrical insulation. In order to improve the insulation performance of the solid insulators, we should consider the following two technical points. Firstly, we have to improve the insulation performance of solid dielectrics itself. The second is the control of the electric field distribution in and around the solid insulating spacers. In this paper, we have proposed a new concept for spacer insulation; an application of a functionally graded material (FGM). We investigated the applicability of FGM for reducing the electric stress on triple junction point, which was one of the important factors dominating a long-term insulating property of the solid. Finite Element Method (FEM) has been used throughout this work, for its favorable accuracy, to calculate the electric field distribution inside gas insulated bus duct (GIBD). The electric field distribution around earthed particle contamination which adhered to uniform and FGM of disc-spacer is studied. Electric field relaxation effect (E_{FGM} / $E_{uniform}$) by introduction of the U-shape FGM spacer is also studied. The breakdown voltage calculations in case of gap with particles contamination are studied. The effect of gas pressure, SF_6-gas concentration in various mixtures and the particle dimension (length and hemi-spherical radius) on the breakdown voltage are also studied. Finally, the effect of FGM of spacer on breakdown voltage is also studied.

Index Terms— Functionally Graded Material (FGM), Finite Element Method (FEM), Electric Field, Particles, Breakdown Voltage.

——————————————— ◆ ———————————————

1 INTRODUCTION

THESE days, electric power equipment tends to be compact and be operated under higher voltage. For the enhancement of insulation reliability and the compact design in gas insulated power equipment, the solid insulators play the crucial role of electrical insulation [1,2]. In order to improve the insulation performance of the solid insulators, we should consider the following two technical points. Firstly, we have to improve the insulation performance of solid dielectrics itself, for example, nano composite material application to the electric power equipment [3,4]. The second is the control of the electric field distribution in and around the solid insulating spacers [5,6].

In the practical gas insulated switchgears, the insulation performance around the spacer are made improved by various techniques, for examples, controlling the spacer shape, adding shield electrodes for electric field relaxation, the introduction of an embedded electrode, and so on. However, these techniques for the control of electric field lead to a more complicated structure of the equipment and increase the manufacturing cost. Thus, it is necessary to propose a new concept on solid spacers with keeping their simple structure and configuration.

We have proposed a new concept for spacer insulation; an application of a functionally graded material (FGM). For relaxation of electric field stress, the FGM spacer should have spatial distribution of dielectric permittivity inside it. By the control of the distribution of dielectric permittivity, we could make the electric field distribution in and around the spacer more suitable. Thus, we have achieved the fundamental inves-

tigations of the FGM spacer in electric power apparatus [7-11]. In this paper, we investigated the applicability of FGM for reducing the electric stress on triple junction point with particle contamination and study its effect on breakdown voltage, which was one of the important factors dominating a long-term insulating property of the solid spacer.

2 PERMITTIVITY DISTRIBUTION IN SOLID SPACER FOR REDUCING ELECTRIC STRESS ON TRIPLE JUNCTION POINT WITH DISC SPACER

2.1 Shape permittivity distribution

In order to relax the electric field stress on electrode surface, the higher permittivity should be given around both anode and cathode surfaces compared with the other intermediate parts of solid insulator. It can be explained by the equivalent capacitor circuits of solid spacer configuration under static field as shown in Fig. 1. The high permittivity capacitors in the vicinity of both sides of electrodes cause potential contingent to the inner low permittivity capacitor, decreasing the electric field in the vicinity of the electrode. Thus, U-shape distribution of the permittivity is suitable for the relaxation of electric field stress on electrode surface [12].
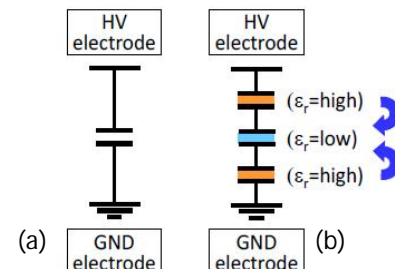

Fig. 1. Equivalent capacitor circuits of solid spacer configuration, (a) uniform permittivity, (b) permittivity distribution for reducing electric field in the vicinity of electrodes.

———————————————
- *Amr A. Youssef, PH.Dresearcher in high voltage engineering, Benha University, Cairo, Egypt. E-mail: eng_power_amr2011@yahoo.com*

2.2 Calculation model for FGM spacer

In order to confirm the field control effect of the proposed distribution of dielectric permittivity, we carried out the numerical calculation of electric field by finite element method (FEM). Fig.2 shows the permittivity distribution (U-shape distribution) for the graded materials. This permittivity distribution was based on the optimized distribution of permittivity for minimizing the electric field stress on triple junction point with disc spacer calculation model by computer-aided optimization technique for the FGM solid insulators. Furthermore, in order to compare the performance, the spacer with uniform permittivity distribution (εr=4.5) was also introduced.
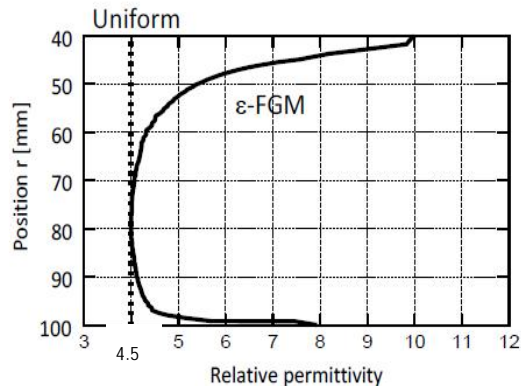

Fig. 2. U-shape permittivity distribution of the spacer [12].

3 ELECTRIC FIELD CALCULATIONS

FEM one of the efficient technique for solving field problems is used to determine the electric field distribution on the spacer's surface. FEM concerns itself with minimization of the energy within the whole field region of interest, whether the field is electric or magnetic, of Laplacian or Poisson type, by dividing the region into triangular elements for two dimensional problems or tetrahedrons for three dimensional problems. Under steady state the electrostatic field within anisotropic dielectric material, assuming a Cartesian coordinate system, and Laplacian field, the electrical energy W stored within the whole volume U of the region considered is [13]:

$$W = \frac{1}{2} \int_U \varepsilon \left| grad(V) \right|^2 dU \tag{1}$$

$$W = \frac{1}{2} \iiint_U \left[\varepsilon_x \left(\frac{\partial V_x}{\partial x} \right)^2 + \varepsilon_y \left(\frac{\partial V_y}{\partial y} \right)^2 + \varepsilon_z \left(\frac{\partial V_z}{\partial z} \right)^2 \right] dxdydz \tag{2}$$

Furthermore, for GIS arrangement, when we consider the field behaviour at minute level the problem can be treated as two dimensional (2D). The total stored energy within this area-limited system is now given according to [13]:

$$\frac{W}{\varphi} = \frac{1}{2} * \varepsilon \iint \left[\left(\frac{\partial V_x}{\partial x} \right)^2 + \left(\frac{\partial V_y}{\partial y} \right)^2 \right] dxdy \tag{3}$$

Where (W/φ) is thus an energy density perelementary area dA. Before applying any minimization criteria based upon the above equation, appropriate assumptions about the potential distribution V(x, y, z) must be made. It should be emphasized that this function is continuous and a finite number of deriva-

tives may exist. As it will be impossible to find a continuous function for the whole area A, an adequate discretization must be made. So all the area under consideration is subdivided into triangular elements hence [13]:

$$\frac{W}{\varphi} = \frac{1}{2} * \varepsilon * \sum_{i=1}^{n} \left[\left(\frac{\partial V_x}{\partial x} \right)^2 + \left(\frac{\partial V_y}{\partial y} \right)^2 \right] * A_i \tag{4}$$

Where n is the total number of elements and Ai is the area of the ith triangle element. So the formulation regarding the minimization of the energy within the complete system may be written as [13]:

$$\frac{\partial X}{\partial \{V(x, y)\}} = 0; \quad Where \quad X = \frac{w}{\varphi} \tag{5}$$

The result is an approximation for the electrostatic potential for the nodes at which the unknown potentials are to be computed. Within each element the electric field strength is considered to be constant and the electric field strength is calculated as [13]:

$$\vec{E} = -\vec{I} \frac{\partial V(x, y)}{\partial x} - \vec{J} \frac{\partial V(x, y)}{\partial y} \tag{6}$$

The electric field is calculated with using the Finite Element Method (FEM) throughout this work. The Finite Element Method Magnetics (FEMM) Package is used to simulate the problems and to calculate the electric field inside gas insulated switchgear and gas insulated bus ducts as disscussed in this paper. FEMM is a finite element package for solving 2D planar and axi-symmetric problems in electrostatics and in low frequency magnetic [14].

The voltage on the high voltage conductor of the configurations considered is taken as 1V, For any applied voltage the values of the electric fields can be proportioned.

3.1 Modeling of Gas Insulated Bus Duct

Gas insulated bus duct consists of aluminum conductor is supported by disc-spacer with the aluminum enclosure as shown in the Fig. 3. All dimensions of gas insulated bus duct with coating and disc-spacer are given in millimeter as shown in the figure. Disc-spacer is made of epoxy material with width 30mm and relative permativity (εr=4.5) or made of FGM which used in this paper. Diameters of the enclosure and conductor are 152mm, 55mm respectively. The void is been filled with SF6 gas. The analysis is done by using two concentric cylinder of infinite length as shown in Fig. 3. The voltage on the inner conductor of GIBD considered is taken as 1V, For any applied voltage the values of the electric fields can be proportioned.
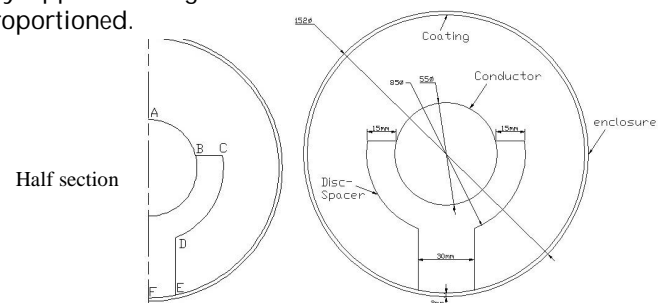

Fig. 3. Gas insulated bus duct with disc-spacer of epoxy material

3.1.1 Electric field distribution along surface of FGM of disc spacer without particle contamination

The electric field distribution along surface of FGM of disc-spacer inside gas insulated bus duct is shown in Fig.4. It is clear that, the electric field increases gradually from lower triple junction point (E) until it reaches a certain value at point (D). From point (D) to point (C) along hemi-spherical radius of disc spacer, the electric field increases and then becomes approximately constant. From point (C) to point (B), the electric field decreases until it reaches minimum value at triple junction point (B) but it returns to increase until it reaches a certain value at point (A) along high voltage conductor.
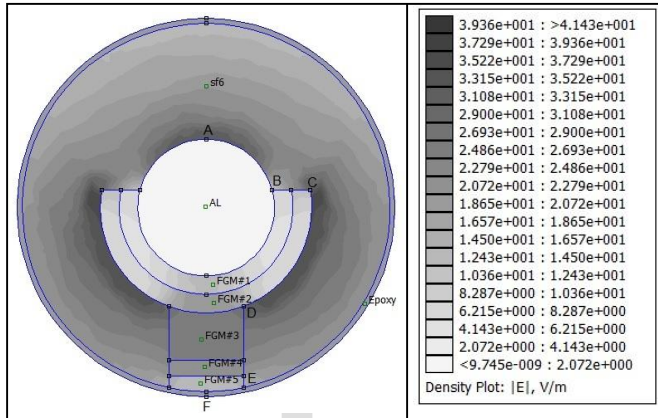

Fig. 4. Electric field distribution along surface of FGM of disc spacer inside gas insulated bus duct.

Fig. 5 shows Electric field distribution along surface of uniform (Epoxy) and FGM of disc spacer inside gas insulated bus duct. It is seen that the electric field decreases gradually from point (A) until it reaches minimum value at point (B) of triple junction point at high voltage conductor. From point (B) to point (C), the electric field increases until it reaches a certain value. From point (C) to point (D), the electric field is approximately constant along hemi-spherical radius of high voltage conductor. From point (D) to point (E), the electric field decreases gradually until it reaches a certain value at triple junction point at ground enclosure. From point (E) to point (F), the electric field is slightly increased. It is found that the electric field strength on the both electrode surfaces in contact with solid insulators was reduced by introduction of the FGM spacers. In addition, the FGM spacer also allowed us to reduce the intensified field strength at distance 38mm and 141mm along (ABCDEF) path at triple junction points (B & E) at high voltage conductor and ground enclosure as shown in the figure.

Fig. 6 shows the electric field relaxation effect on the electrode/spacer interface ($=E_{FGM}/E_{uniform}$). The result shows a relaxation effect of 0.69 on high voltage electrode/spacer interface and 0.75 on ground electrode/spacer interface by applying the U-shape FGM spacer.
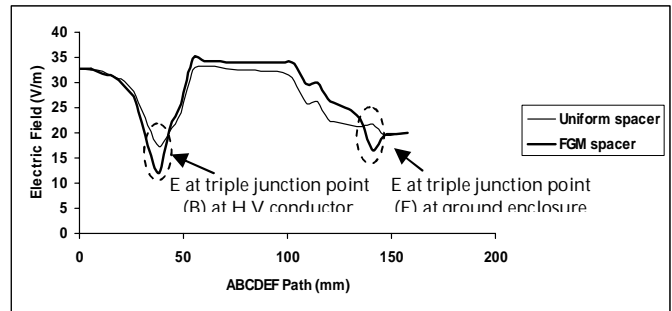

Fig. 5. Electric field distribution along surface of uniform (Epoxy) and FGM of disc spacer inside gas insulated bus duct.
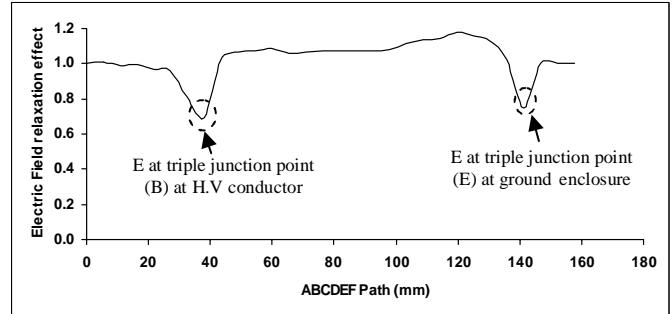

Fig. 6. Electric field relaxation effect (E_{FGM} / $E_{uniform}$) by introduction of the U-shape FGM spacer.

3.1.2 Electric field distribution along surface of FGM of disc spacer with single contaminating particle adhered to spacer

Fig. 7 shows gas insulated bus duct with FGM of disc spacer and single contaminating particle of Aluminum (Al.) adhered to spacer. Particle length (L) and radius (r) are taken as 5mm and 0.5mm respectively. Gu is defined as upper gap space from triple junction point of particle up to high voltage conductor.
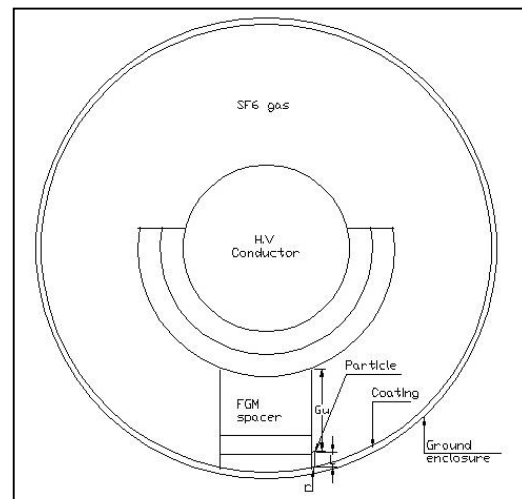

Fig. 7. Gas insulated bus duct with FGM of disc spacer and single contaminating particle adhered to spacer.

Fig. 8 shows the electric field distribution along surface of FGM of disc-spacer with single contaminating particle adhered to spacer inside gas insulated bus duct. From this figure, it can be observed that, the electric field increases gradually from lower tip point (a) of particle until it reaches maximum value at triple junction point (c). From point (c) up to high voltage conductor, the electric field decreases gradually through gap as far from particle until it reaches a certain value and then it slightly increased as it approached from high voltage conductor.
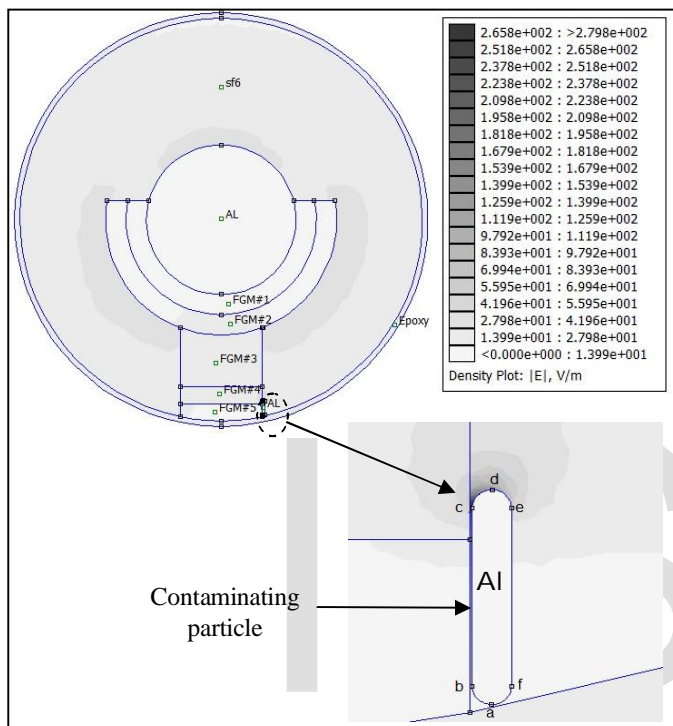

Fig. 8. Electric field distribution along surface of FGM of disc spacer with single contaminating particle adhered to spacer inside gas insulated bus duct.

Electric field distribution along particle length which adhered to uniform (Epoxy) or FGM of disc spacer is shown in Fig.9. It seen that the electric field increases gradually from minimum value at lower tip point (a) of particle until it reaches maximum value at triple junction point (c) but after that point, it decreases gradually through path (d-e-f) until it reaches the minimum value at lower tip point (a). From this figure, also it can be observed that the electric field is reduced at triple junction point(c) of particle with FGM spacer than it with uniform (Epoxy) spacer. Hence the field intensification at triple junction point (c) of particle is reduced by applying the U-shape FGM spacer.

Fig. 10 shows electric field distribution along upper gap space from triple junction point (c) of particle up to high voltage conductor. From this figure, it is found that the electric field decreases from maximum value at triple junction point (c) as far from particle until it reaches a certain value but after that point it slightly increased as it approached from high voltage conductor. The maximum electric field at triple junction point (c) of particle is reduced by about 10% with applying U-shape FGM spacer than it with uniform (Epoxy) spacer.
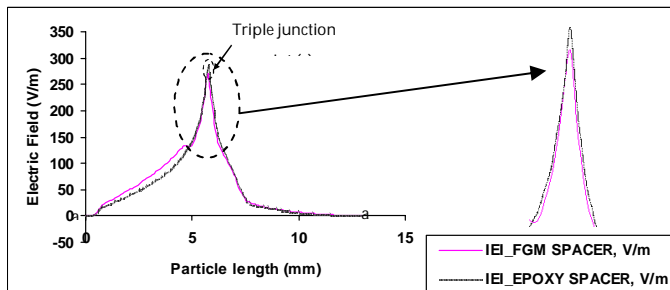

Fig. 9. Electric field distribution along particle length which adhered to uniform (Epoxy) or FGM of disc spacer.
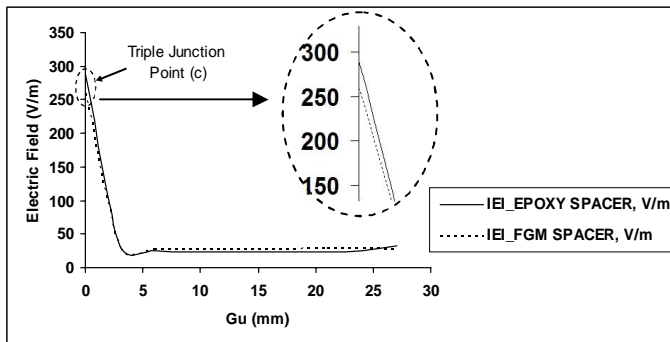

Fig. 10. Electric field distribution along upper gap space from triple junction point (c) of particle up to high voltage conductor.

4 IONIZATION COEFFICIENTS FOR SF₆-GAS MIXTURES

In order to compute the breakdown voltages of SF_6 – gas mixtures, a knowledge of the effective ionization coefficient $\bar{\propto}$ as a function of the electric field intensity (E) in the neighborhood of $\bar{\propto}$ =0 is a prerequisite. The net ionization coefficients for SF_6 –gas mixtures ($\bar{\propto}$)mix can be calculated from the values of $\bar{\propto}$ in pure gases. For pure Nitrogen the net ionization coefficients $\bar{\propto}$ can be approximated by [15];

$$\frac{\bar{\propto}}{P}=66\exp\left[\frac{-2.15}{E/P}\right] \tag{7}$$

The measurements of the effective ionization coefficient $\bar{\propto}$ for CO_2 has been summarized by Rein and can be approximated by the following equations [16] :

$$\frac{\bar{\propto}}{P}=176.5\exp\left[\frac{-2.565}{E/P}\right] \qquad \text{for } 0.2<=E/P<=0.28 \tag{8}$$

$$\frac{\bar{\propto}}{P}=50.3\exp\left[\frac{-1.515}{E/P}\right] \qquad \text{for } 0.28<E/P<=100 \tag{9}$$

For air, the ionization coefficients can be approximated by [17],

$$\frac{\bar{\propto}}{P}=22\left(E/P-0.244\right)^2 \qquad \text{for } 0.244<E/P<=0.5 \tag{10}$$

$$\frac{\bar{\propto}}{P}=15.8114\left(E/P-0.244\right)^{1.75} \qquad \text{for } 0.5<E/P<=1.2 \tag{11}$$

For pure SF_6, $\bar{\propto}$ /P can be expressed as [18],

$$\frac{\bar{\propto}}{P}=27\left(E/P-0.8775\right) \tag{12}$$

In Eqs. (7) through (12) , P is the gas pressure in kPa , $\bar{\propto}$ /P is given in $(cm.kPa)^{-1}$ and E/P has the units of $kV(cm.kPa)^{-1}$.

For a given SF_6-gas mixture, the effective ionization coefficient is assumed to be given by :

$$(\bar{\propto}/P)mix=F(\bar{\propto}/P)SF_6+(1-F)(\bar{\propto}/P)gas \qquad (13)$$

where, $F = P(SF_6) / P(mix)$ is the partial pressure ratio of the SF_6 component in a given gas mixture.

When added two electronegative gases to SF_6-gas mixture, the effective ionization coefficient is assumed to be given by :

$$(\bar{\propto}/P)mix=F1(\bar{\propto}/P)SF_6+F2(\bar{\propto}/P)gas_1+F3(\bar{\propto}/P)gas_2 \qquad (14)$$

where, $F1=P(SF_6)/P(mix)$ is the partial pressure ratio of the SF_6 component in a given gas mixture, $F2=P(gas_1)/P(mix)$ is the partial pressure ratio of the first electronegative gas in a given gas mixture and $F3=P(gas_2)/P(mix)$ is the partial pressure ratio of the second electronegative gas in a given gas mixture.

5 METHODOLOGY FOR BREAKDOWN VOLTAGE CALCULATIONS

In order to study the breakdown voltages for a particle which is represented by a hemi-spherical tip with diameter (2r) and length (L) which is contaminating inside gas insulated bust duct for SF_6 - gas mixture under DC voltage. The electric field around particles is satisfied in this paper by using finite element method.

With an applied electric field, discharges in the gas occur as a result of ionization, which lead to streamer formation and ultimately to breakdown of the gas mixture. One way to predict breakdown voltage of the gas mixture is, therefore, by knowing its effective ionization coefficient.

In a non-uniform field gap, corona discharges will occur when the conditions for a streamer formation in the gas are fulfilled. Streamer formation is both pressure and field dependent, and therefore depends on the electrode profile, geometry of the contaminating particle, its position in the gap between electrodes if it is free, and on the instantaneous value of the ambient field. The condition for streamer formation is given by;

$$\int_{0}^{xc} \bar{\propto}(x)dx \geq K \qquad (15)$$

Where, $\bar{\propto}(x)=\alpha(x)-\eta(x)$, $\alpha(x)$ and $\eta(x)$ are the first ionization coefficient and the coefficient of attachment, respectively; both being functions of field and thus of geometry.

The distance (xc) from the particle's tip or triple junction point is where the net ionization is zero, normally known as the ionization boundary. There is some controversy over the value of K, the discharge constant. The value of K for pure gases in the pressure range of 100 to 400 kPa is obtained as follows using the breakdown data given in CIGRE paper [19];

In this study for breakdown voltages we take the value of

K = 18.42 for SF_6 gas and SF_6 - gas mixture but K=5 for N_2 gas and K=27 for CO_2 gas [20].

6 BREAKDOWN VOLTAGE CALCULATIONS FOR GAS MIXTURES WITH PARTICLE CONTAMINATION

Figs. 11,12 show breakdown voltage in the gap of gas insulated bus duct with FGM spacer and particle contamination of length (5mm) and radius (0.5mm) which adhered to spacer.

Fig. 11 shows the effect of gas pressure on the breakdown voltage for various fractional concentrations of SF_6-CO_2-Air gas mixtures. We fixed the fractional concentration of SF_6 gas at 5% in these mixtures with various fractional concentrations of CO_2 and Air to avoid disadvantages of SF_6 gas such as high costs and also obtain the optimum gas mixture. From this figure, it can be observed that, the breakdown voltage for (SF_6-CO_2-Air) increases when fractional concentration of SF_6 gas is constant at 5% and with increasing fractional concentration of CO_2 gas and with decreasing fractional concentration of Air. Also, the breakdown voltage for mixture is increased as the pressure of mixture increases. From these mixtures, the optimum gas mixture is observed at 5%SF_6-80%CO_2-15%Air.

Fig. 12 shows the effect of gas pressure on the breakdown voltage for various fractional concentrations of SF_6-N_2-Air gas mixtures. We fixed the fractional concentration of SF_6 gas at 5% in these mixtures with various fractional concentrations of N_2 and Air to avoid disadvantages of SF_6 gas such as high costs and also obtain the optimum gas mixture. From this figure, it can be observed that, the breakdown voltage for (SF_6-N_2-Air) increases when fractional concentration of SF_6 gas is constant at 5% and with increasing fractional concentration of N_2 gas and with decreasing fractional concentration of Air. Also, the breakdown voltage for mixture is increased as the pressure of mixture increases. From these mixtures, the optimum gas mixture is observed at 5%SF_6-80%N_2-15%Air.

From Fig. 11 and Fig. 12, the optimum gas mixture which preferred to be used is 5%SF_6-80%N_2-15%Air.

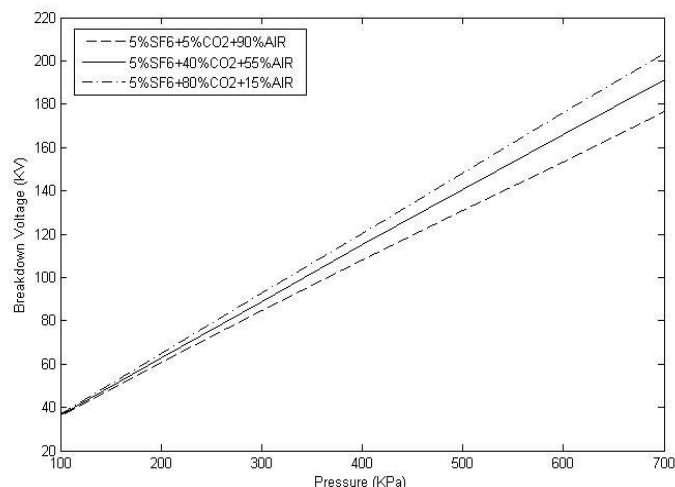Fig. 11. Effect of gas pressure on the breakdown voltage for various fractonal concentrations of SF_6-CO_2–Air gas mixtures.
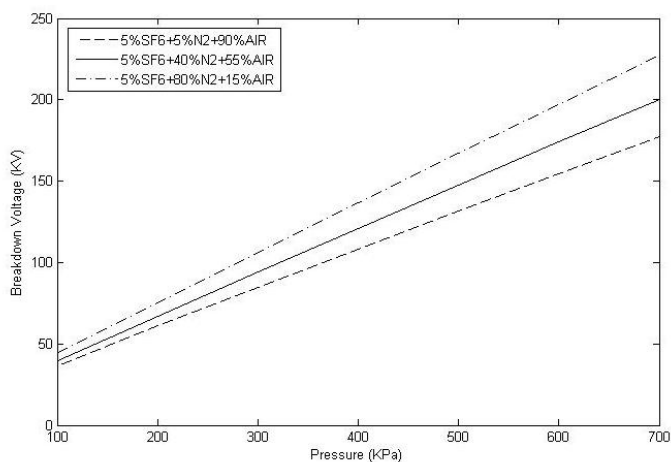
Fig. 12. Effect of gas pressure on the breakdown voltage for various fractional concentrations of SF_6-N_2–Air gas mixtures.

Fig. 13 shows the effect of uniform and functional graded material (FGM) of spacer on the breakdown voltage. From this figure, it can be observed that breakdown voltage in case of FGM of spacer is greater than it in case of uniform (epoxy) spacer. By application of functional graded material of spacer, the breakdown voltage is increased by about 10%.
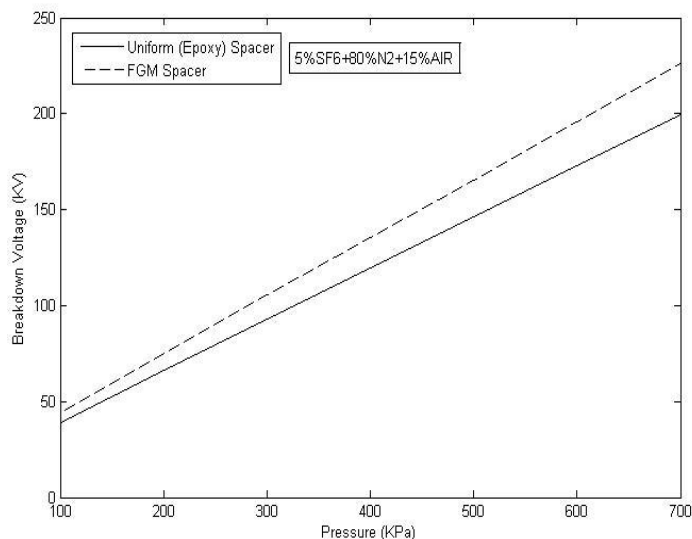

Fig. 13. Effect of uniform and functional graded material (FGM) of spacer on Breakdown Voltage.

Fig. 14 shows the effect of particle length on the breakdown voltage for various fractional concentrations of SF_6-N_2-Air mixtures at constant radius 0.5mm and pressure 500kPa. From this figure, it can be observed that the breakdown voltage of $5\%SF_6$-$80\%N_2$-$15\%Air$ gas mixture is greater than it of $5\%SF_6$-$40\%N2$-$55\%Air$ gas mixture which is greater than it of $5\%SF_6$-$5\%N2$-$90\%Air$ mixture, so $5\%SF_6$-$80\%N_2$-$15\%Air$ gas mixture is still the optimum gas mixture at different values of particle length. Also, as particle length increases, the breakdown voltage decreases.

Fig. 15 shows the effect of particle radius on the breakdown voltage for various fractional concentrations of SF_6-N_2-Air

mixtures at constant particle length 5mm and pressure 500kPa. From this figure, it can be observed that the breakdown voltage of $5\%SF_6$-$80\%N_2$-$15\%Air$ gas mixture is greater than it of $5\%SF_6$-$40\%N_2$-$55\%Air$ gas mixture which is greater than it of $5\%SF_6$-$5\%N_2$-$90\%Air$ mixture, so $5\%SF_6$-$80\%N_2$-$15\%Air$ gas mixture is still the optimum gas mixture at different values of particle radius. Also, as particle radius increases, the breakdown voltage increases also.
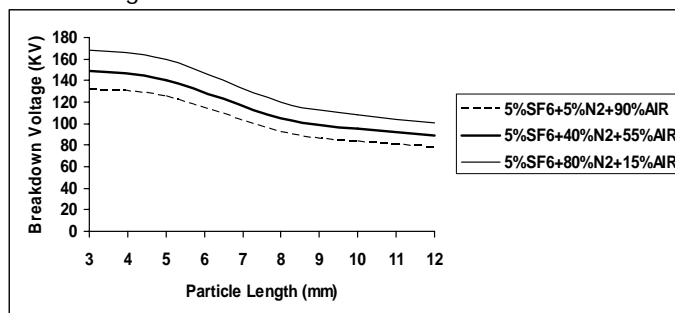

Fig. 14. Effect of particle length on the breakdown voltage for various fractional concentrations of SF_6-N_2-Air mixtures.
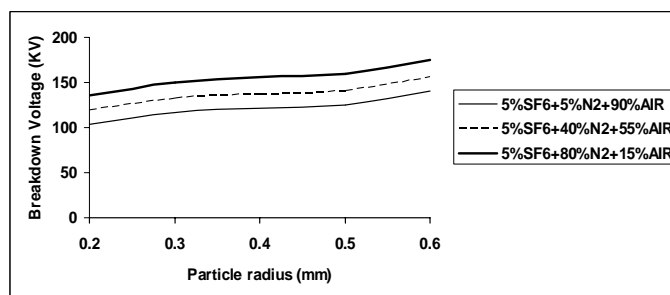

Fig. 15. Effect of particle radius on the breakdown voltage for various fractional concentration of SF_6-N_2-Air mixtures.

7 CONCLUSIONS

In this study, electrostatic modeling of gas insulated bus duct which represented by two concentric cylinder of infinite length which supported by disc spacer with different materials of insulator and with contaminating particles are presented. From this work, it can be observed that the electric field is maximum value at triple junction point of particle which adhered to spacer and this value decreases gradually as far from particle until it reaches a certain point but it returns to increase slightly as near to high voltage conductor. In this paper, a new concept on solid spacers with keeping their simple structure and configuration is used. An application of a functionally graded material (FGM) is applied to disc spacer to reduce the concentration of the maximum electric field at triple junction point of particle with spacer and gas which was one of the important factors dominating a long-term insulating property of the solid spacer. When it compared the effect of FGM spacer with uniform (Epoxy) spacer in case of gap without any particle contamination, it can be observed that the electric field at triple junction points which in contact with high voltage conductor and with ground enclosure in case of FGM spacer are reduced than it in case of Epoxy spacer. The electric field relaxation effects of 0.69 on high voltage electrode/spacer interface and 0.75 on ground electrode/spacer interface by applying the U-shape FGM spacer. The maximum electric field at

triple junction point of particle which adhered to spacer is reduced by about 10% with applying U-shape FGM spacer than it with uniform (Epoxy) spacer. The breakdown voltage for mixture is increased as the pressure of mixture increases. We fixed the fractional concentration of SF_6 gas at 5% in the mixtures with various fractional concentrations of N_2, CO_2 and Air to avoid disadvantages of SF_6 gas such as high costs and also obtain the optimum gas mixture. From different gas mixtures, the optimum gas mixture is observed at $5\%SF_6$-$80\%N_2$-15%Air. By application of functional graded material of spacer, the breakdown voltage is increased by about 10%. The breakdown voltage increases as particle radius increases or as particle length decreases. Finally, we advised to use FGM spacer instead of uniform (Epoxy) spacer in case of practical gas insulated bus duct for its great advantages to reduce field concentration at triple junction point which considered the dangerous point at gas insulated bus duct and can lead to breakdown the gas.

REFERENCES

[1]   CIGRE WG 15.03: "LONG-TERM PERFORMANCE OF SF6 INSULATED SYSTEMS", *CIGRE Report* 15-301, 2002.

[2]   T. Tanaka, T. Okamoto, K. Nakanishi and T. Miyamoto, "Aging and Related Phenomena in Modern Electric Power Systems", *IEEE Trans.Dielectr. Electr. Insul.*, Vol. 28, No.5, pp.826-844, 1993.

[3]   M. F. Fréchette, C. W. Reed: "The Emerging Field of Nanodielectrics:an Annotated Appreciation", *IEEE Intern. Sympos. Electr. Insul. (ISEI)*, pp.458-465, 2006.

[4]   T. Tanaka, Y. Ohki, M. Ochi, M. Harada and T. Imai, "Enhanced Partial Discharge Resistance of Epoxy/Clay Nanocomposite Prepared by Newly Developed Organic Modification and Solubilization Methods", *IEEE Trans. Dielectr. Electr. Insul.*, Vol. 15, No.1, pp.81-89, 2008.

[5]   A. Haddad and D. Warne, "dvances in High Voltage Engineering", *The Institution of Electrical Engineers UK*, 2004.

[6]   S. Okabe, N. Hayakawa, H. Murase, H. Hama, and H. Okubo, "Common Insulating Properties in Insulating Materials", *IEEE Trans. Dielectr. Electr. Insul.*, Vol. 13, pp.327-335, 2006.

[7]   M. Kurimoto, K. Kato, H. Adachi, S. Sakuma, H. Okubo, "Fabrication and experimental verification of permittivity graded solid spacer for GIS", *IEEE Conf. Electr. Insul. Dielectr. Phenomena (CEIDP)*, pp. 789-792, 2002.

[8]   H. Okubo, M. Kurimoto, H. Shumiya, K. Kato, H. Adachi, S. Sakuma, "Permittivity Gradient Characteristics of GIS Solid Spacer", *IEEE 7th Intern. Conf. Properties and Applications of Dielectric Materials(ICPADM)*, pp. 23-26, 2003.

[9]   H. Shumiya, K. Kato and H. Okubo, "Feasibility Study on FGM (Functionally Graded Materials) Application for Gas Insulated Equipment", *IEEE Conf. Electr. Insul. Dielectr. Phenomena (CEIDP)*, pp.360-363, 2004.

[10] K. Kato, M. Kurimoto, H. Shumiya, H. Adachi, S. Sakuma and H.Okubo, "Application of Functionally Graded Material for Solid Insulator in Gaseous Insulation System", *IEEE Trans. Dielectr. Electr. Insul.*, Vol. 13, pp.362-372, 2006.

[11] H. Okubo, H. Shumiya, M. Ito and K. Kato, "Optimization Techniques on Permittivity Distribution in Permittivity Graded Solid Insulators", *IEEE Intern. Sympos. Electr. Insul. (ISEI)*, pp.519-522, 2006.b

[12] M.A. Abd Allah, Sayed A. Ward, Amr A. Youssef, "Effect of Functionally Graded Material of Disc Spacer with Presence of Multi-Contaminating Particles on Electric Field inside Gas Insulated Bus Duct", *International Journal of Electrical and Computer Engineering (IJECE)*, Vol. 3, No. 6, pp.831-848, 2013.

[13] E. Kuffel, W.S. Zaengl and J. Kuffel, "High Voltage Engineering Fundamentals", *Second edition, Butterworth-Heinemann Linacre House, Jordan Hill, Oxford OX2 8DP, 225 Wildwood Avenue, Woburn, MA01801-2041*, pp. 246-254, 2000.

[14] David Meeker, "Finite Element Method Magnetics, Version 4.2, User's Manual", September 2006.

[15] N. H. Malik, A. H. Qureshi, "A review of electrical breakdown in mixtures of SF6 and other gases", *IEEE Transaction on Electrical Insulation*, Vol. EI- 14, No. 1, pp. 1-13, 1979.

[16] A Rein, " Breakdown mechanisms and breakdown criteria in gases: Measurement of discharge parameters. A literature survey", *Bioctra*, No. 32, pp. 43-60, 1974.

[17] S. Berger, "Onset of breakdown voltage reduction by electrode surface roughness in air and SF6", *IEEE Trans. on PAS, Vol. PAS-95*, No. 4, pp. 1073-1079, 1976.

[18] N. H. Malik and A. H. Qureshi, "Breakdown mechanisms in sulphur-hexafluoride", *IEEE Trans. on Elect. Insul.*, Vol. EI-12, No. 3, pp. 135-145, 1978.

[19] T.W. Dakin, G. Luxa, G. Oppermann, J. Vigreux, G. Wind, H. Winkeln- Kemper, "Breakdown of gases in uniform fields, Paschen curves for nitrogen, air and sulphur-hexaflouride", *Electra. CIGRE* Paper No.32, pp.64-70, 1974.

[20] Sayed A. Ward, M. A. Abd Allah, Amr A. Youssef, " Multi-Particle Initiated Breakdown of Gas Mixtures inside Compressed Gas Devices", E*lectric*al *Insulation and Dielectric Phenomena (CEIDP) Conference, IEEE,* pp. 353-356, 2012.